A Monte Carlo model for reactor antineutrino's spectrum

Lorenzo Loi

Research advisors
Prof. Antonio Cammi
Prof. ssa Monica Sisti
Prof. Davide Chiesa

Politecnico di Milano - INFN Milano Bicocca - Roma Tre JUNO Italia meeting

March 29, 2023

Overview

1. Introduction
2. Takahama validation
3. Results
   - C/E
   - Axial distribution
   - Fission fraction
4. Conclusions

Background

Nuclear reactors are adopted as antineutrino sources due to the massive β^- emitters produced during burnup. The reactor antienutrino spectrum can be estimated by:

Background

Nuclear reactors are adopted as antineutrino sources due to the massive β^- emitters produced during burnup. The reactor antienutrino spectrum can be estimated by:

- **Conversion method**: calculated integral spectra from the four fissionables are combined to find the total rate.

Background

Nuclear reactors are adopted as antineutrino sources due to the massive β^- emitters produced during burnup. The reactor antienutrino spectrum can be estimated by:

- **Conversion method**: calculated integral spectra from the four fissionables are combined to find the total rate.
- **Ab-initio method**: the antienutrino spectrum is predicted by the knowledge of the four actinides fraction and by their associated emission spectra, weighted over the yield production.

$$S_\nu(E,t) = \sum_i f_i(t) S_{\nu,i}(E)$$

$$i \in \{^{235}\mathrm{U}, ^{238}\mathrm{U}, ^{239}\mathrm{Pu}, ^{241}\mathrm{Pu}\}$$

- f_i fission fraction;
- $S_{\nu,i}$ weighted sum of antineutrino spectra emitted by fissile isotope i.

Fission fractions

Simulation codes are able to track the time evolution of both the neutron flux Φ and also the fission reaction rate $\Phi \cdot \sigma_{f,i}$, allowing the **fission fraction estimation** over a given period.

$$\mathbf{f_i(t)} = \frac{\int \Phi(\mathbf{r}, E, T, t)\sigma_{f,i}(E,T)\, dx^3 dE}{\sum_i \int \Phi(\mathbf{r}, E, T, t)\sigma_{f,i}(E,T)\, dx^3 dE}$$

The fission fractions are integral quantities, whose singular value depends by:

- The fresh fuel composition;
- The rate at which the fuel is being depleted (i.e., the power).

The flux and nuclide field are quantities highly linked within each others. The correct prediction of the latter represents the approximation degree of the former.

Post Irradiation Experiment

Monte Carlo codes are able to perform very *detailed* reactor analysis. The neutronic prediction's accuracy can be tested by comparing isotopic concentrations. **Post Irradiation Experiments** (PIE) allow to have a map of nuclide field map in spent fuel storage through radiochemical analysis.

Post Irradiation Experiment

Monte Carlo codes are able to perform very *detailed* reactor analysis. The neutronic prediction's accuracy can be tested by comparing isotopic concentrations. **Post Irradiation Experiments** (PIE) allow to have a map of nuclide field map in spent fuel storage through radiochemical analysis.
Spent fuel data were available from the Takahama-3 Light Water Reactor. The experiment is summarized as follows:

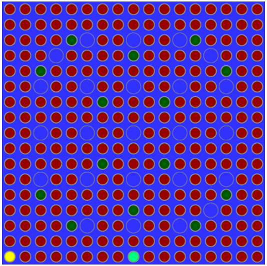

Figure 1: Takahama XY view.

- Two fuel rods (SF95, SF97) were placed in two 17x17 assemblies and depleted for ∼ **875** and ∼ **1370** days;
- At the end of the burnup period, the rods were placed in decay pool for 4 years;

Post Irradiation Experiment

- Then, slices of 0.5 mm were extracted at several height (5 samplings for SF95 and 6 for SF97)

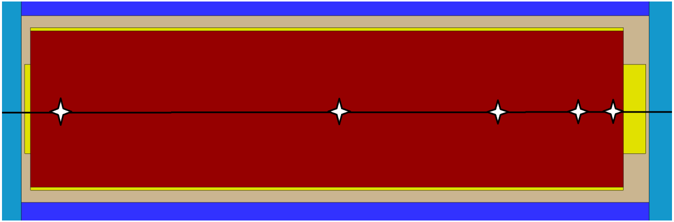

Figure 2: SF95 samples.

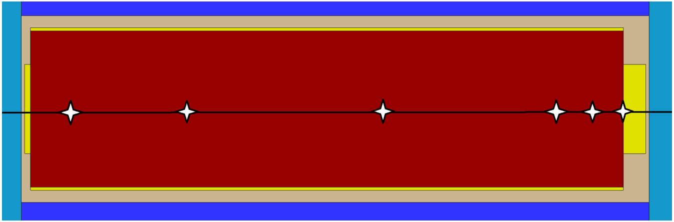

Figure 3: SF97 samples.

Measured nuclides

For each sample, up to 35 concentration were measured and adjusted at the discharge time from the assembly.

Isotope	Measurement Technique	Maximum standard deviation
^{234}U	IDMS	1 %
$\mathbf{^{235}U}$, $\mathbf{^{238}U}$	IDMS	0.1 %
^{236}U	IDMS	2 %
^{238}Pu	IDMS	0.5 %
$\mathbf{^{239}Pu}$, ^{240}Pu, $\mathbf{^{241}Pu}$, ^{242}Pu	IDMS	0.3 %
Nd, Sm isotopes	IDMS	0.1 %
^{241}Am, ^{243}Cm, ^{244}Cm	αs, MS	2 %
^{243}Am, ^{246}Cm	αs, MS	5 %
^{242m}Am, ^{242}Cm, ^{247}Cm	αs, MS	10 %
Gd isotopes	MS	0.1 %
^{237}Np	αs	10 %
^{134}Cs, ^{137}Cs, ^{154}Eu	γs	3 %
^{106}Ru	γs	5 %
^{125}Sb , ^{144}Ce	γs	10 %

Measured nuclides

For each sample, up to 35 concentration were measured and adjusted at the discharge time from the assembly.

Isotope	**Measurement Technique**	**Maximum standard deviation**
^{234}U	IDMS	1 %
$\mathbf{^{235}U}$, $\mathbf{^{238}U}$	IDMS	0.1 %
^{236}U	IDMS	2 %
^{238}Pu	IDMS	0.5 %
$\mathbf{^{239}Pu}$, ^{240}Pu, $\mathbf{^{241}Pu}$, ^{242}Pu	IDMS	0.3 %
Nd, Sm isotopes	IDMS	0.1 %
^{241}Am, ^{243}Cm, ^{244}Cm	αs, MS	2 %
^{243}Am, ^{246}Cm	αs, MS	5 %
^{242m}Am, ^{242}Cm, ^{247}Cm	αs, MS	10 %
Gd isotopes	MS	0.1 %
^{237}Np	αs	10 %
^{134}Cs, ^{137}Cs, ^{154}Eu	γs	3 %
^{106}Ru	γs	5 %
^{125}Sb , ^{144}Ce	γs	10 %

Among those, this analysis focuses on the four fissile species ^{235}U, ^{239}Pu, ^{238}U and ^{241}Pu.

C/E

The prediction capability will be evaluated with the *calculated-to-experimental* ratio:

$$C/E_i = \frac{N_i^C}{N_i^E} \pm \sigma_i(exp) \tag{1}$$

where N_i^C and N_i^E represent the calculated and measured concentration of the isotope i in a sample position and $\sigma_i(exp)$ is the uncertainty associated to the measurement procedure.

C/E

The prediction capability will be evaluated with the *calculated-to-experimental* ratio:

$$C/E_i = \frac{N_i^C}{N_i^E} \pm \sigma_i(exp) \tag{1}$$

where N_i^C and N_i^E represent the calculated and measured concentration of the isotope i in a sample position and $\sigma_i(exp)$ is the uncertainty associated to the measurement procedure.

We aim to investigate **how precisely the Monte Carlo simulation is able to predict the local nuclide field** with the approximation of:

- Constant fuel temperature at 900 K;
- Piecewise fuel temperature at 750 K, 900 K and 1200 K.

Modelling features

The two rods were modelled in three ways each:

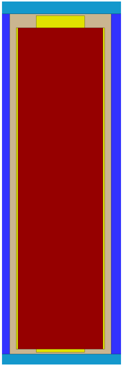

Figure 4: 1 dep. zone, 1 temperature.

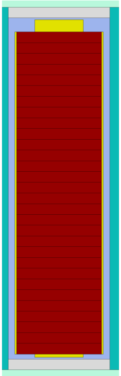

Figure 5: 30 dep. zones, 1 temperature.

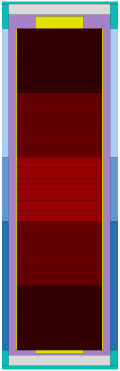

Figure 6: 30 dep. zone, 5 temperatures.

C/E - SF95

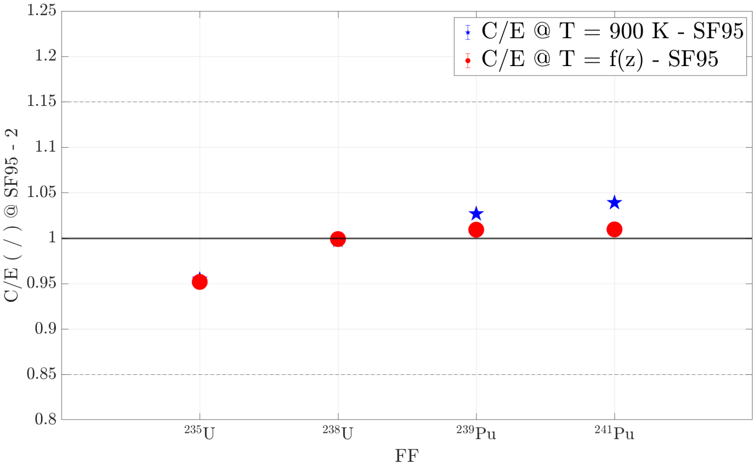

Figure 7: SF95 - 2 (C/E)

C/E - SF95

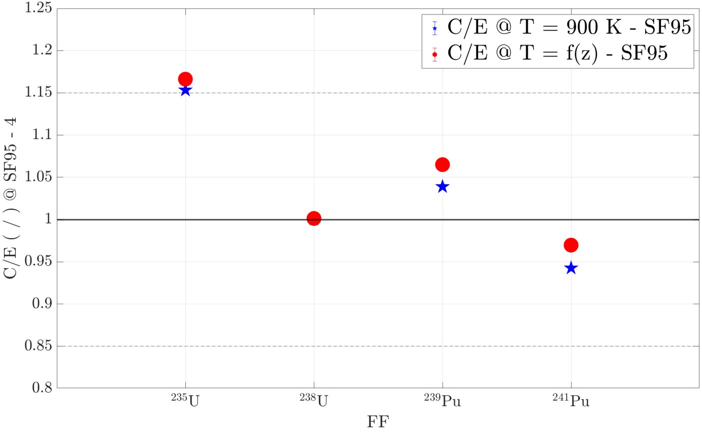

Figure 8: SF95 - 4 (C/E)

C/E - SF95

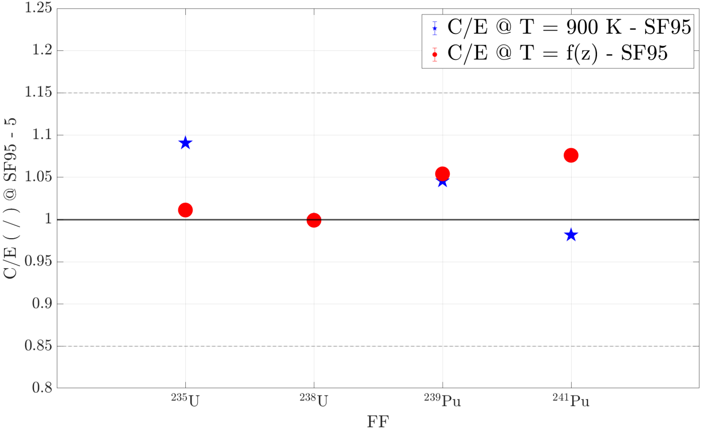

Figure 9: SF95 - 5 (C/E)

C/E - SF97

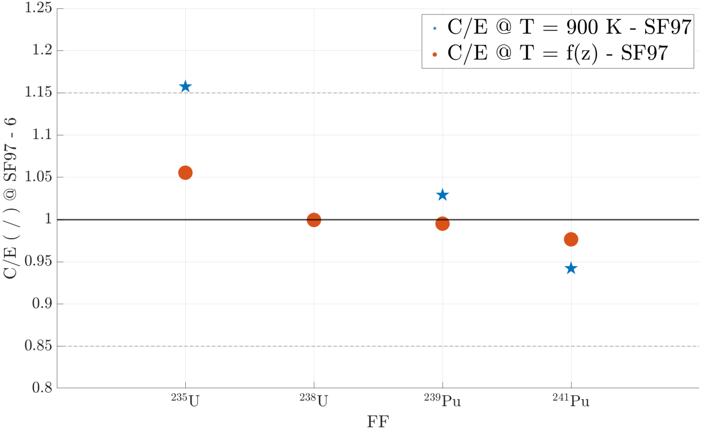

Figure 10: SF97 - 6 (C/E)

C/E - SF97

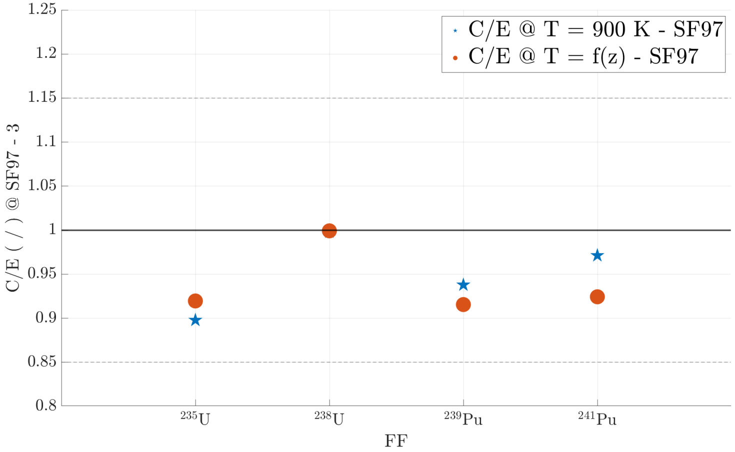
C/E @ T = 900 K - SF97
C/E @ T = f(z) - SF97
C/E (/) @ SF97 - 3
1.25
1.2
1.15
1.1
1.05
1
0.95
0.9
0.85
0.8
^{235}U
^{238}U
^{239}Pu
^{241}Pu
FF

C/E - SF97

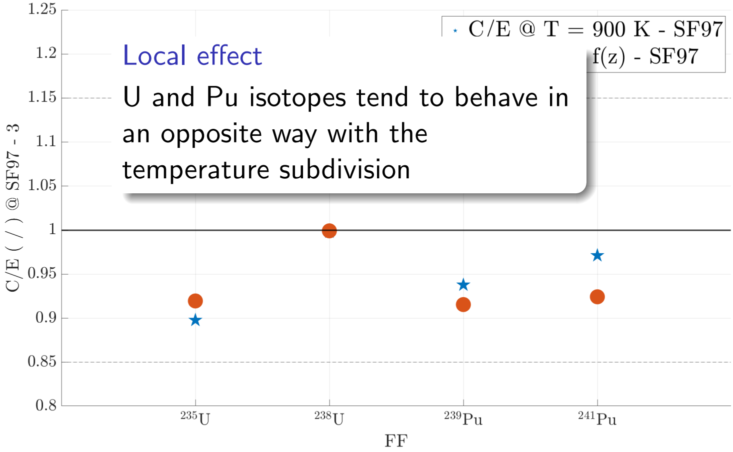

Local effect

U and Pu isotopes tend to behave in an opposite way with the temperature subdivision

Axial distribution - SF97

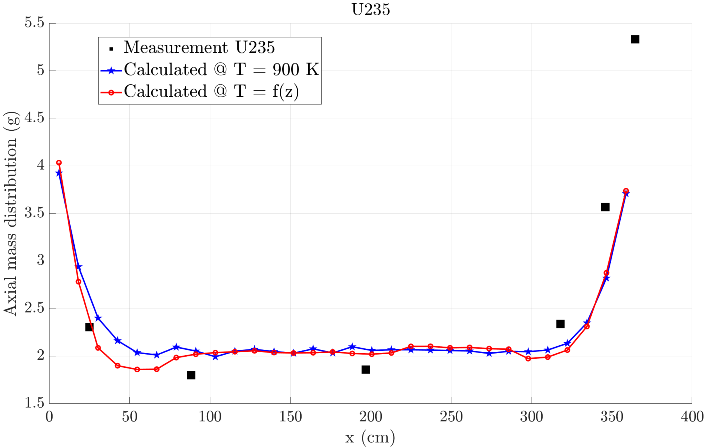

Figure 11: Axial comparison - U235

Axial distribution - SF97

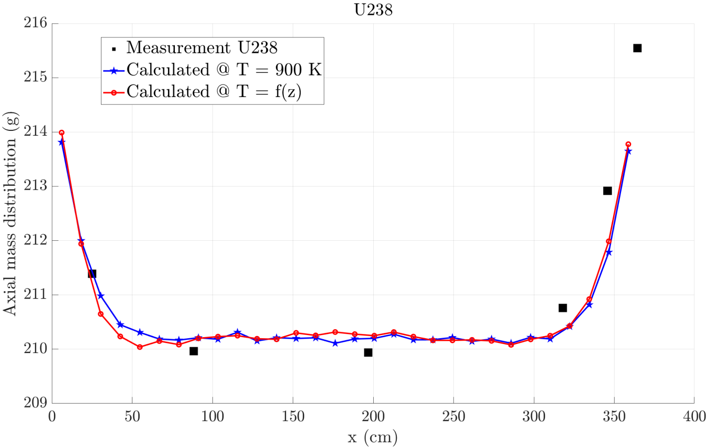

Figure 12: Axial comparison - U238

Axial distribution - SF95

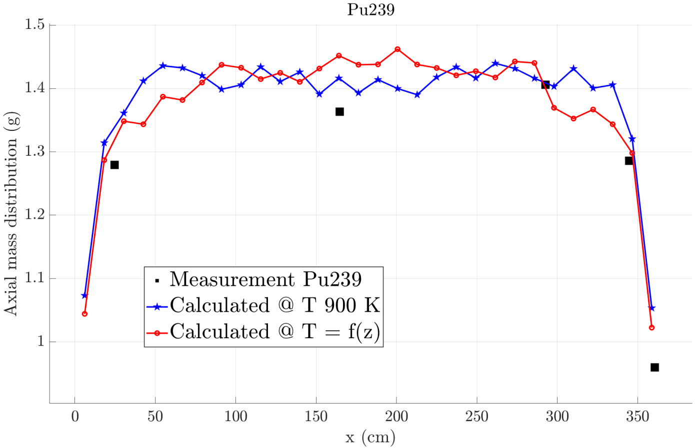

Figure 13: Axial comparison - Pu239

Axial distribution - SF95

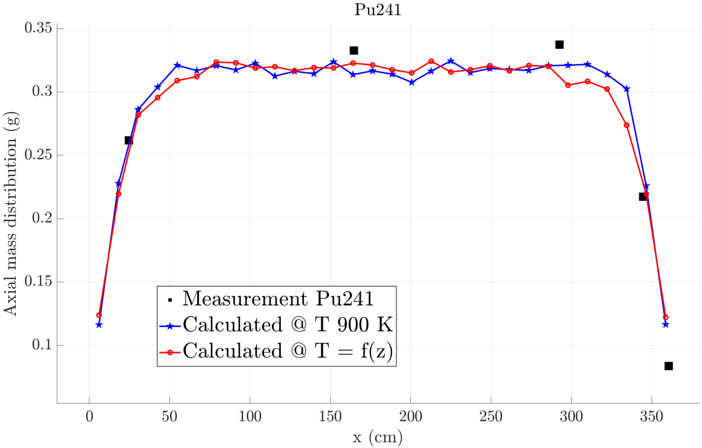

Figure 14: Axial comparison - Pu241

Axial distribution - SF97

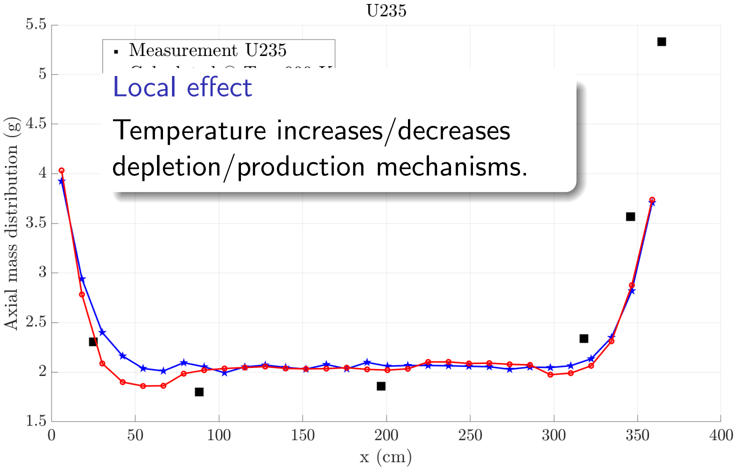

Local effect

Temperature increases/decreases depletion/production mechanisms.

Fission fraction evolution - SF97

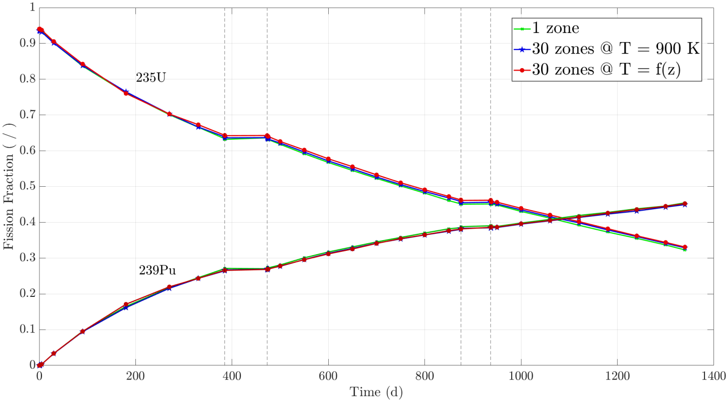

Figure 15: FF evolution comparison - 235 and 239

Fission fraction evolution - SF97

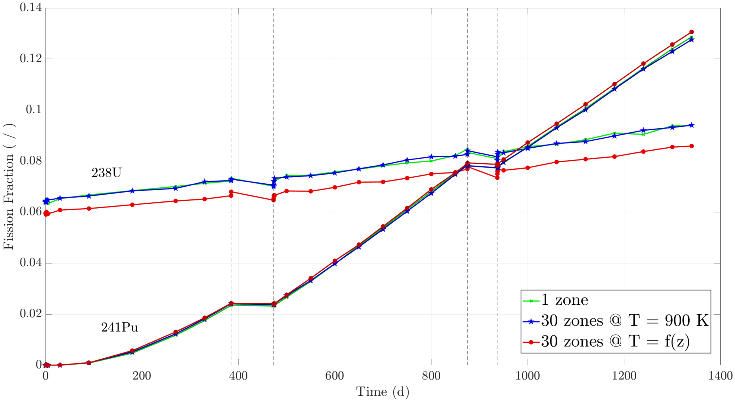

Figure 16: FF evolution comparison - 238 and 241

Fission fraction difference

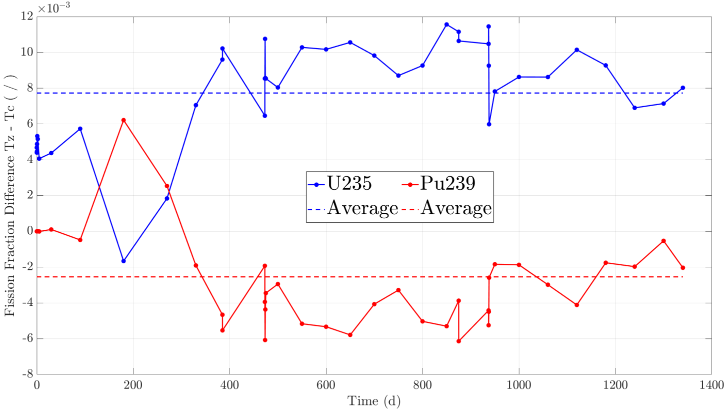

Figure 17: FF evolution comparison - difference 235 and 239

Fission fraction difference

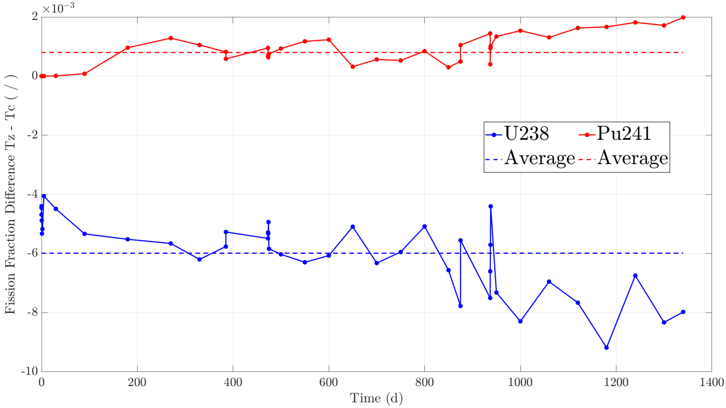

Fission fraction difference

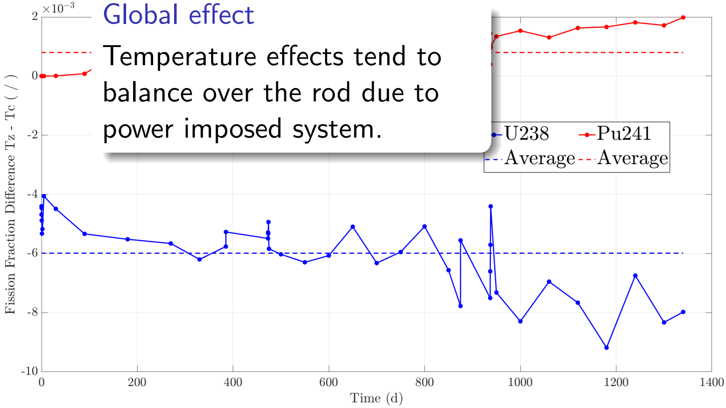

Global effect

Temperature effects tend to balance over the rod due to power imposed system.

Conclusions

- The Monte Carlo simulation techniques is able to estimate the four main fissile isotopes within $5 - 15\%$ of the experimental data;
- The temperature effect plays a major role **locally**, increasing or decreasing the depletion/production rate of the fuel region;
- However, the temperature effect tend to *balance* due to the power imposed framework: the fission fraction evolution of the whole system shows a sub-percent difference in the two temperature environments.

Thank you for the attention!
Questions?